

Computational Tools

Exploring the Dynamics of Cell Processes through Simulations of Fluorescence Microscopy Experiments

Juan Angiolini,¹ Nicolas Plachta,^{2,3} Esteban Mocskos,^{4,5,*} and Valeria Levi^{1,*}

¹Departamento de Química Biológica-IQUIBICEN, Facultad de Ciencias Exactas y Naturales, Universidad de Buenos Aires, Buenos Aires, Argentina; ²European Molecular Biology Laboratory, Australian Regenerative Medicine Institute, Monash University, Victoria, Australia; ³Institute of Molecular and Cell Biology, A*STAR, Singapore; ⁴Departamento de Computación, Facultad de Ciencias Exactas y Naturales, Universidad de Buenos Aires, Buenos Aires, Argentina; and ⁵Centro de Simulación Computacional p/Aplicaciones Tecnológicas, CSC-CONICET, Buenos Aires, Argentina

ABSTRACT Fluorescence correlation spectroscopy (FCS) methods are powerful tools for unveiling the dynamical organization of cells. For simple cases, such as molecules passively moving in a homogeneous media, FCS analysis yields analytical functions that can be fitted to the experimental data to recover the phenomenological rate parameters. Unfortunately, many dynamical processes in cells do not follow these simple models, and in many instances it is not possible to obtain an analytical function through a theoretical analysis of a more complex model. In such cases, experimental analysis can be combined with Monte Carlo simulations to aid in interpretation of the data. In response to this need, we developed a method called FERNET (Fluorescence Emission Recipes and Numerical routines Toolkit) based on Monte Carlo simulations and the MCell-Blender platform, which was designed to treat the reaction-diffusion problem under realistic scenarios. This method enables us to set complex geometries of the simulation space, distribute molecules among different compartments, and define interspecies reactions with selected kinetic constants, diffusion coefficients, and species brightness. We apply this method to simulate single- and multiple-point FCS, photon-counting histogram analysis, raster image correlation spectroscopy, and two-color fluorescence cross-correlation spectroscopy. We believe that this new program could be very useful for predicting and understanding the output of fluorescence microscopy experiments.

INTRODUCTION

Fluorescence correlation spectroscopy (FCS) methods (1–7) are widely used to explore the dynamics of biological processes (8). FCS consists of the analysis of intensity fluctuations caused by fluorescently labeled molecules moving through the small observation volume of a confocal or two-photon excitation microscope. Since the temporal window of these fluctuations is given by the processes that determine the mobility of the molecules and their photophysics, this technique has been extensively applied to study diffusion, transport, chemical reactions, etc. (reviewed in Elson (9)). Analysis of fluorescence intensity fluctuations also provides the local concentration of fluorescent molecules and their brightness, which can be used to detect the formation of molecular complexes (10,11). The great innovations made in fluorescence fluctuation measurements will probably produce new and useful approaches to be applied to an increasingly wide range of subjects (8).

For simple cases, such as molecules following Brownian motion, FCS analysis yields analytical functions that can be fitted to the experimental data to recover the phenomenological parameters (e.g., diffusion coefficients and chemical rate constants). Unfortunately, many dynamical processes

in cells do not follow these simple models, and in many instances it is not possible to obtain an analytical function through a theoretical analysis of a more complex model (9). In such cases, the analysis can be combined with Monte Carlo simulations (for example, see Dix et al. (12) and the SimFCS program from the Laboratory for Fluorescence Dynamics, University of California, Irvine (UCI), Irvine, CA; <http://www.lfd.uci.edu/globals/>). A comparison of experimental data and the predictions of a reduced, simulated model could provide important clues about the dynamical processes hidden in the FCS data.

Most of the Monte Carlo methods used to simulate FCS experiments consist of ad hoc tools designed for specific scenarios, which makes it difficult for an inexperienced user to adapt the routine to a different situation. Moreover, these routines usually assume homogeneous systems and do not allow inclusion of a user-defined geometry (12,13), which is necessary to describe, for example, the complex architecture of cells.

In this work, we present FERNET (Fluorescence Emission Recipes and Numerical routines Toolkit), a new, to our knowledge, toolkit we designed to simulate the output of a variety of FCS-based techniques in user-defined scenarios. This program works in combination with the MCell-Blender platform (14–16), which was designed to treat the reaction-diffusion problem under realistic

Submitted November 19, 2014, and accepted for publication April 9, 2015.

*Correspondence: emocskos@dc.uba.ar or vlevi12@gmail.com

Editor: David Rueda.

© 2015 by the Biophysical Society
0006-3495/15/06/2613/6 \$2.00



<http://dx.doi.org/10.1016/j.bpj.2015.04.014>

scenarios. The program can be used on standard desktop computers with no special hardware requirements, and allows the user to define the architecture of the space and reactions among species, opening up a wide range of possible simulation scenarios. We believe that this new program will be useful for predicting and interpreting the output of fluorescence fluctuation experiments.

MATERIALS AND METHODS

Simulation of dynamical processes

MCell is a tool that was designed to capture the complexity involved in biological processes such as signaling and metabolic pathways, which include interactions between various components in solution and/or in structures. This program has several advantages with respect to other simulation tools because the standard approximation for reaction-diffusion systems ignores the discrete nature of the reactants and the stochastic character of their interactions, whereas techniques based on the chemical master equation, such as the Gillespie algorithm (17), assume that at each instant the particles are uniformly distributed in space.

The MCell package (<http://mcell.org>) includes optimized routines to support Brownian dynamics to model the diffusion of individual molecules in volumes or surfaces, ray tracing of random walk motion vectors to detect collisions among molecules, ray marching to propagate rays after collisions, and Monte Carlo probabilities to decide which collisions lead to reaction events (14–16). The particles move diffusively and it is assumed that if a reaction exists, it follows a Poisson process and happens instantaneously. This allows one to decouple the reaction event from the diffusive motion of the particle. The time step of the algorithm is determined such that only single particles or pairs of particles have to be considered, avoiding complex reaction rules.

To deal with the definition of the complex environment for the simulation, MCell is combined with CAD program Blender (<http://www.blender.org>) using the CellBlender plugin. Blender provides a broad spectrum of modeling, texturing, lighting, animation, and video postprocessing functionalities in one package. The combination of these tools allows one to create realistic 3D scenarios that can be used to simulate the complexity of the underlying biological processes.

Obtaining fluorescence intensity traces with FERNET

FERNET generates fluorescence intensity traces and images from MCell simulations according to the algorithm schematized in Fig. 1. For the simulations presented in this work, we considered a Gaussian confocal volume; however, the size of the observation volume can be easily modified, as indicated in File S1 in the Supporting Material. At every simulation time step, the program evaluates the position of each particle and calculates the probability of emission (g) as follows (5):

$$g(x, y, z) = \exp\left(\frac{-2((x - x_0)^2 + (y - y_0)^2)}{\omega_{xy}^2} + \frac{-2(z - z_0)^2}{\omega_z^2}\right), \quad (1)$$

where ω_{xy} and ω_z are the radial and axial waists of the point spread function (PSF), respectively, and (x_0, y_0, z_0) is the center of the confocal volume.

To determine whether the molecule is excited, the value of g is compared with a random number between 0 and 1; if the former is greater, the molecule is considered to be promoted to an excited state. To determine whether

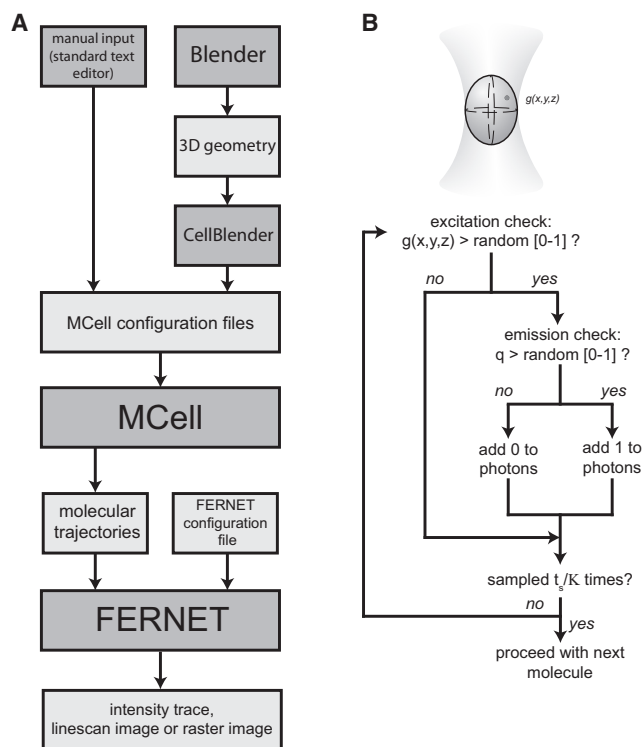


FIGURE 1 (A and B) Schematic representation of the MCell-FERNET workflow (A) and FERNET routine (B).

the excited molecule emits photons, a random number between 0 and 1 is compared with the value of q , defined as $q = \epsilon' \cdot \kappa$, where ϵ' is the molecular brightness (in counts per second per molecule) and κ is the dwell time between emission events. The molecule emits if the random number is higher than q . The user can set the values of ϵ and κ as desired; we included as default parameters $\epsilon' = 10^5$ cpsm and $\kappa = 200$ ns (12).

To determine the number of photons emitted by the molecule during the sampling time set by the user (t_s), the program repeats this last step t_s/κ times, assuming that the position of the simulated molecule is approximately constant during t_s . This statement may not be true for fast-moving molecules; therefore, the program compares t_s with the mean residency time for the fastest molecule (τ_D): if $\tau_D < 10 t_s$, the program suggests that t_s be modified to correctly sample the simulated system.

This procedure is repeated with all of the molecules at every simulation time step, and the intensity trace is then calculated by adding up the photons emitted by the molecules at each time step.

To ensure that the fluorescence experiments were simulated in the equilibrium condition, we first ran MCell, let the system evolve to equilibrium, and set the obtained concentration of the species as initial parameters for the MCell-FERNET routine.

Correlation functions and photon-counting histogram analysis

Correlation functions and photon-counting histograms (PCHs) were calculated from the simulated intensity traces using specific correlation software (SimFCS; Laboratory for Fluorescence Dynamics, UCI) or custom-made MATLAB (The MathWorks, Natick, MA) routines.

The correlation function was calculated as

$$G_{ij}(\tau) = \frac{\langle \delta I_i(t) \cdot \delta I_j(t + \tau) \rangle}{\langle I_i(t) I_j(t) \rangle}, \quad (2)$$

where $\delta I(t) = I(t) - \langle I(t) \rangle$ represents the fluctuation of the intensity (I), the brackets indicate the time average, and τ is the lag time. The subscripts i and j refer to the detection channels. If $i = j$, then G_{ii} represents the autocorrelation function (ACF), whereas $i \neq j$ corresponds to the cross-correlation function (CCF).

RESULTS AND DISCUSSION

We first ran simulations of molecules passively diffusing in a 3D homogeneous medium and calculated the ACF and PCH from the intensity trace recovered in this simple simulation condition (Fig. 2). The continuous lines in the figure represent the best fit of the PCH obtained by using the theoretical PCH function (11) and the fitting of the ACF data to the equation expected for 3D Brownian diffusion (18):

$$G(\tau) = \frac{\gamma}{N} \frac{1}{\left(1 + \frac{4D\tau}{\omega_o^2}\right) \sqrt{\left(1 + \frac{4D\tau}{z_o^2}\right)}}, \quad (3)$$

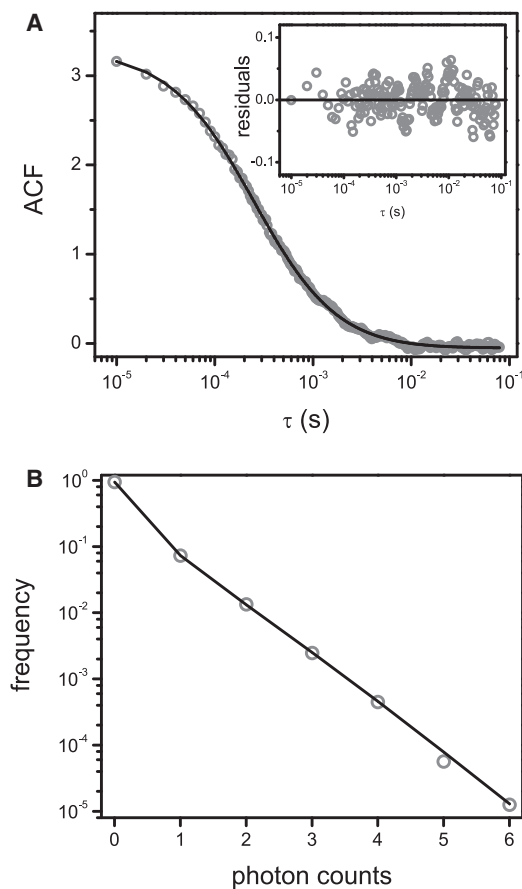


FIGURE 2 Simulation of FCS routines. (A and B) Single-point FCS: a simulation of 300 molecules ($\epsilon = 10^5$ cpsm) passively moving with $D = 40 \mu\text{m}^2/\text{s}$ in a cube (side length = $6 \mu\text{m}$) was run with $t_s = 10 \mu\text{s}$ during 100 s. The ACF (A) and PCH (B) data calculated from the intensity trace obtained with the FERNET routine were fitted as described in the text (continuous lines), resulting in the parameters detailed in Table 1.

where D is the diffusion coefficient of the molecules, τ is the lag time, N is the mean number of molecules in the confocal volume, γ is a geometric factor that depends on the detection profile for a Gaussian volume $\gamma = 0.35$ (18), and ω_o and z_o are the radial and axial waists of the PSF, respectively.

Table 1 shows that both the diffusion coefficient (D) and brightness of molecules (ϵ) are correctly recovered, illustrating the robustness of the routine presented in this work for single-point FCS measurements.

To show the extra possibilities provided by the ability of MCell to create spatial features, we defined two compartments separated by a permeable barrier (Fig. S1 A in the Supporting Material) and considered different diffusion coefficients and brightness levels for molecules in each compartment. Thus, whenever a molecule moves from one compartment to the other (e.g., when moving between cellular compartments with different rheological properties), the diffusion coefficient changes. This process was simulated as a reaction occurring on the membrane: every time a molecule hit the membrane, there was a probability of destroying this molecule and creating a second one with different D and ϵ values at the same position on the other side of the membrane.

We then calculated the ACF and PCH curves at different positions of the sample as could be done using different multifocal FCS techniques (2,19,20). Fig. S1 shows pseudo-color images of the D , N , and ϵ values recovered at every analyzed position either by fitting Eq. 3 to the ACFs or by PCH analysis. These maps closely resemble the simulated data, with the exception of the positions intersecting the barrier, which presented intermediate values as expected.

FERNET also includes the possibility of moving the observation volume, allowing simulations of both the image acquisition (Movie S1) and different scanning-FCS routines (1,5–7). Fig. S2 shows the results obtained in a simulated raster-image correlation spectroscopy (RICS) experiment (12). We fitted the correlation matrix as shown in Digman et al. (6) and obtained the expected values of D and N (Table 1).

Two-color cross-correlation FCS (FCCS) is powerful extension of FCS that allows one to detect interactions between molecules (reviewed in Bacia et al. (4)). Thus,

TABLE 1 Simulated and recovered parameters of PCH and RICS analyses

| Experiment | Parameter | Simulation | Correlation | |
|------------------|----------------------------------|------------|------------------|-----------------|
| | | | Analysis | PCH Analysis |
| Single-point FCS | D ($\mu\text{m}^2/\text{s}$) | 40.00 | 39.79 ± 0.35 | – |
| | N | 0.31 | 0.29 ± 0.01 | 0.31 ± 0.01 |
| | ϵ (cpm) | 1.00 | – | 0.92 ± 0.02 |
| RICS | D ($\mu\text{m}^2/\text{s}$) | 40 | 40.72 ± 0.56 | – |
| | N | 0.27 | 0.28 ± 0.01 | – |

Values are expressed as mean \pm standard error from 10 independent simulations.

we included in the program the possibility of simulating multicolor measurements (see configuration details in Document S2).

To illustrate how this tool could be used to explore interactions, we considered different scenarios involving the binding of molecules to fixed targets. Previous works showed that such simulations are extremely helpful for exploring the interaction of transcription factors (TFs) with chromatin in living cells (13,21). First, we analyzed simple cases in which two molecules (e.g., different TFs labeled with spectrally well-separated fluorophores) interacted with different binding sites (Fig. 3 A) or competed for the same targets (Fig. 3 B). While the ACFs of the two molecules were very similar and showed the diffusion ($\tau_{\text{diff}} \sim 0.2\text{--}0.5$ ms) and binding ($\tau_{\text{binding}} \sim 10$ ms) components expected according to Michelman-Ribeiro et al. (13), these different scenarios could be clearly distinguished through the cross-correlation analysis.

To show how the versatility of MCell allows one to include user-defined reactions, we considered other interactions that may affect the binding of molecules with targets. In the first case, molecule A (red circle in Fig. 3 C) interacts with molecule B (green rectangle in Fig. 3 C), and the A-B complex binds to the target. This case is similar to a TF whose DNA-binding efficiency is influenced by its interaction with other proteins (e.g., the estrogen receptor requires calmodulin to bind DNA (22,23). Fig. 3 C shows that the CCF presents two components that are compatible with the free diffusion of complexes and their binding to the targets. Also, we simulated a sequential recruitment of A and B to the binding site (e.g., the glucocorticoid receptor bound to chromatin recruits co-regulators involved in receptor-mediated promoter activation (24). The ACFs obtained for the green and red channels were different due to the sequential

binding of molecules (Fig. 3 D). In addition, there was a clear, positive cross correlation in a timescale compatible with the binding process.

Recent improvements in microscopy cameras have resulted in more efficient detection and higher acquisition speeds, allowing the simultaneous and parallel collection of intensity traces with a millisecond time resolution. This development constitutes the basis of imaging-FCS, in which microscopy techniques such as total internal reflection fluorescence microscopy and selective plane illumination microscopy, which confines the excitation to a thin z section of the sample, are combined with FCS (25–27). Given the relevance of these new techniques, we also included in the program the possibility of simulating FCS experiments with camera detection (Fig. S3).

The above examples illustrate how the program can help the user to predict the results of FCS experiments, to rationalize how relevant information can be extracted from experiments, and to understand how different parameters of either the system or the data acquisition could influence the output of the experiments.

For a correct interpretation of the experimental data, these analyses should be combined with an adequate selection of the model based on a strict statistical study that also considers the influence of noise in fluorescence fluctuation measurements and cell-to-cell variability. In recent years, the Bathe group (25,26,28) has developed a Bayesian inference procedure for testing multiple competing models to describe temporal ACFs. This procedure enables the systematic and objective evaluation of different models for FCS data, appropriately penalizing model complexity as the signal/noise ratio decreases.

This group also proposed a statistical blocking procedure (25) that can be easily applied to experimental data to

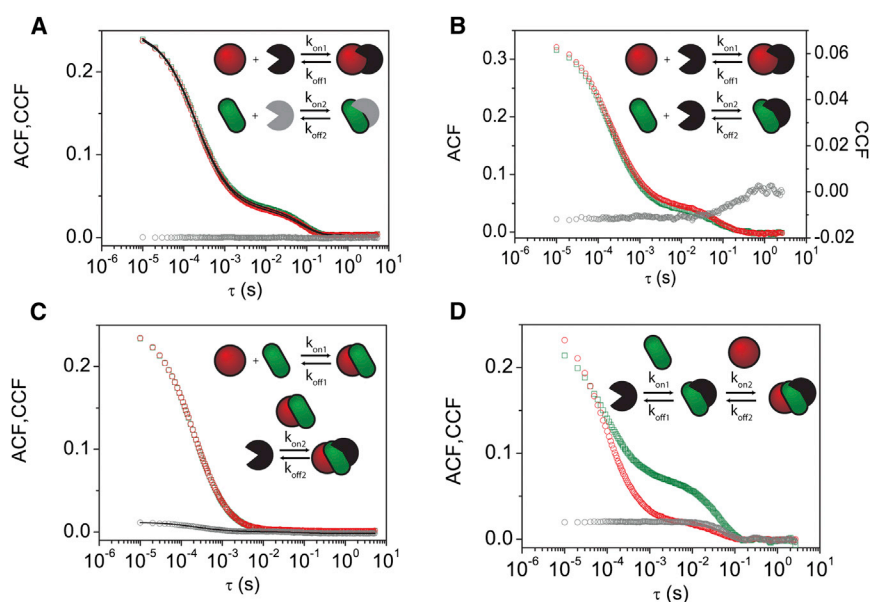


FIGURE 3 Detecting interactions with two-color FCS. Simulations of two-color FCS experiments were run considering two populations of molecules tagged with spectrally separated fluorescent probes (depicted as red circles and green rectangles). The fluorescence intensity of these molecules was assumed to be collected in independent channels (red and green symbols, respectively). (A–D) The ACFs of the intensity obtained for the red (\circ) and green (\square) channels, and the CCFs (gray symbols) were calculated for the following scenarios: (A) noncompetitive binding, (B) competitive binding, (C) complex formation and binding, and (D) sequential binding. The diffusion and binding model proposed by Michelman-Ribeiro et al. (13) was fitted to the ACF and CCF curves in those scenarios in which the assumptions of the model were fulfilled (continuous lines). The simulated and recovered parameters are summarized in Table S1. To see this figure in color, go online.

properly estimate the correlated noise present in ACF curves. This step is essential for an unbiased model selection and parameter estimation.

CONCLUSION

In this work, we have presented, to our knowledge, a new simulation platform based on MCell that allows one to simulate advanced fluorescence microscopy experiments. Because of the easy-to-program options provided by MCell, the MCell-FERNET platform could also be adapted to include a wide variety of photochemical and photophysical processes such as photobleaching and/or photoswitching reactions (12,29), binding to uniform or asymmetrically organized targets (Movie S1), and complex interactions among molecules. We believe that this program could be extremely useful for predicting and understanding the output of fluorescence microscopy experiments.

FERNET and the customized version of MCell can be downloaded from our website (<http://www.dc.uba.ar/FERNET>).

SUPPORTING MATERIAL

Three figures, one table, user manual of FERNET toolkit, one movie, and one zip file containing the parameters used for the simulations presented in Fig. 3 are available at [http://www.biophysj.org/biophysj/supplemental/S0006-3495\(15\)00393-8](http://www.biophysj.org/biophysj/supplemental/S0006-3495(15)00393-8).

AUTHOR CONTRIBUTIONS

E.M., N.P., and V.L. designed research. J.A. and E.M. programmed the custom version of MCell and FERNET. J.A., V.L., and E.M. performed the simulations and data analysis. J.A., E.M., N.P., and V.L. wrote the manuscript.

ACKNOWLEDGMENTS

This research was supported by ANPCyT (PICT 2012-0899) and UBACyT (20020110100074). N.P. is supported by a Viertel Foundation Senior Medical Research Fellowship and NHMRC grants APP1052171 and APP1062263. E.M. and V.L. are members of CONICET.

REFERENCES

- Ruan, Q., M. A. Cheng, ..., W. W. Mantulin. 2004. Spatial-temporal studies of membrane dynamics: scanning fluorescence correlation spectroscopy (SFCS). *Biophys. J.* 87:1260–1267.
- Dertinger, T., V. Pacheco, ..., J. Enderlein. 2007. Two-focus fluorescence correlation spectroscopy: a new tool for accurate and absolute diffusion measurements. *ChemPhysChem*. 8:433–443.
- Burkhardt, M., and P. Schwille. 2006. Electron multiplying CCD based detection for spatially resolved fluorescence correlation spectroscopy. *Opt. Express*. 14:5013–5020.
- Bacia, K., S. A. Kim, and P. Schwille. 2006. Fluorescence cross-correlation spectroscopy in living cells. *Nat. Methods*. 3:83–89.
- Hebert, B., S. Costantino, and P. W. Wiseman. 2005. Spatiotemporal image correlation spectroscopy (STICS) theory, verification, and application to protein velocity mapping in living CHO cells. *Biophys. J.* 88:3601–3614.
- Digman, M. A., C. M. Brown, ..., E. Gratton. 2005. Measuring fast dynamics in solutions and cells with a laser scanning microscope. *Biophys. J.* 89:1317–1327.
- Hinde, E., F. Cardarelli, ..., E. Gratton. 2010. In vivo pair correlation analysis of EGFP intranuclear diffusion reveals DNA-dependent molecular flow. *Proc. Natl. Acad. Sci. USA*. 107:16560–16565.
- Elson, E. L. 2013. 40 years of FCS: how it all began. *Methods Enzymol.* 518:1–10.
- Elson, E. L. 2011. Fluorescence correlation spectroscopy: past, present, future. *Biophys. J.* 101:2855–2870.
- Chen, Y., J. D. Müller, ..., E. Gratton. 2002. Molecular brightness characterization of EGFP in vivo by fluorescence fluctuation spectroscopy. *Biophys. J.* 82:133–144.
- Chen, Y., J. D. Müller, ..., E. Gratton. 1999. The photon counting histogram in fluorescence fluctuation spectroscopy. *Biophys. J.* 77:553–567.
- Dix, J. A., E. F. Hom, and A. S. Verkman. 2006. Fluorescence correlation spectroscopy simulations of photophysical phenomena and molecular interactions: a molecular dynamics/monte carlo approach. *J. Phys. Chem. B*. 110:1896–1906.
- Michelman-Ribeiro, A., D. Mazza, ..., J. G. McNally. 2009. Direct measurement of association and dissociation rates of DNA binding in live cells by fluorescence correlation spectroscopy. *Biophys. J.* 97:337–346.
- Stiles, J. R., D. Van Helden, ..., M. M. Salpeter. 1996. Miniature end-plate current rise times less than 100 microseconds from improved dual recordings can be modeled with passive acetylcholine diffusion from a synaptic vesicle. *Proc. Natl. Acad. Sci. USA*. 93:5747–5752.
- Kerr, R. A., T. M. Bartol, ..., J. R. Stiles. 2008. Fast Monte Carlo simulation methods for biological reaction-diffusion systems in solution and on surfaces. *SIAM J. Sci. Comput.* 30:3126.
- Stiles, J. R., and T. M. Bartol. 2001. Monte Carlo methods for simulating realistic synaptic microphysiology using MCell. In *Computational Neuroscience: Realistic Modeling for Experimentalists*. E. De Schutter, editor. CRC Press, Boca Raton, pp. 87–127.
- Gillespie, D. 1976. A general method for numerically simulating the stochastic time evolution of coupled chemical reactions. *J. Comput. Phys.* 22:403–434.
- Lakowicz, J. R. 2006. *Principles of Fluorescence Spectroscopy*. Springer, New York.
- Kannan, B., J. Y. Har, ..., T. Wohland. 2006. Electron multiplying charge-coupled device camera based fluorescence correlation spectroscopy. *Anal. Chem.* 78:3444–3451.
- Sisan, D. R., R. Arevalo, ..., J. S. Urbach. 2006. Spatially resolved fluorescence correlation spectroscopy using a spinning disk confocal microscope. *Biophys. J.* 91:4241–4252.
- Mazza, D., T. J. Stasevich, ..., J. G. McNally. 2012. Monitoring dynamic binding of chromatin proteins in vivo by fluorescence correlation spectroscopy and temporal image correlation spectroscopy. *Methods Mol. Biol.* 833:177–200.
- Cifuentes, E., J. M. Mataraza, ..., G. P. Reddy. 2004. Physical and functional interaction of androgen receptor with calmodulin in prostate cancer cells. *Proc. Natl. Acad. Sci. USA*. 101:464–469.
- Li, L., Z. Li, and D. B. Sacks. 2005. The transcriptional activity of estrogen receptor- α is dependent on Ca²⁺/calmodulin. *J. Biol. Chem.* 280:13097–13104.
- Ratman, D., W. Vanden Berghe, ..., K. De Bosscher. 2013. How glucocorticoid receptors modulate the activity of other transcription factors: a scope beyond tethering. *Mol. Cell. Endocrinol.* 380:41–54.
- Guo, S. M., N. Bag, ..., M. Bathe. 2014. Bayesian total internal reflection fluorescence correlation spectroscopy reveals hIAPP-induced plasma membrane domain organization in live cells. *Biophys. J.* 106:190–200.

26. Guo, S. M., J. He, ..., M. Bathe. 2012. Bayesian approach to the analysis of fluorescence correlation spectroscopy data II: application to simulated and in vitro data. *Anal. Chem.* 84:3880–3888.
27. Wohland, T., X. Shi, ..., E. H. Stelzer. 2010. Single plane illumination fluorescence correlation spectroscopy (SPIM-FCS) probes inhomogeneous three-dimensional environments. *Opt. Express.* 18:10627–10641.
28. He, J., S. M. Guo, and M. Bathe. 2012. Bayesian approach to the analysis of fluorescence correlation spectroscopy data I: theory. *Anal. Chem.* 84:3871–3879.
29. Kolin, D. L., S. Costantino, and P. W. Wiseman. 2006. Sampling effects, noise, and photobleaching in temporal image correlation spectroscopy. *Biophys. J.* 90:628–639.

Biophysical Journal

Supporting Material

Exploring the Dynamics of Cell Processes through Simulations of Fluorescence Microscopy Experiments

Juan Angiolini,¹ Nicolas Plachta,^{2,3} Esteban Mocskos,^{4,5,*} and Valeria Levi^{1,*}

¹Departamento de Química Biológica-IQUIBICEN, Facultad de Ciencias Exactas y Naturales, Universidad de Buenos Aires, Buenos Aires, Argentina; ²European Molecular Biology Laboratory, Australian Regenerative Medicine Institute, Monash University, Victoria, Australia; ³Institute of Molecular and Cell Biology, A*STAR, Singapore; ⁴Departamento de Computación, Facultad de Ciencias Exactas y Naturales, Universidad de Buenos Aires, Buenos Aires, Argentina; and ⁵Centro de Simulación Computacional p/Aplicaciones Tecnológicas, CSC-CONICET, Buenos Aires, Argentina

SUPPORTING MATERIAL

TABLE SI

| Scenario | Parameter | Simulation | ACF/CCF analysis |
|-------------------------------|---|------------|------------------|
| Non-competitive binding | $D_{\text{red}} (\mu\text{m}^2/\text{s})$ | 50.00 | 50.21 ± 0.16 |
| | $D_{\text{green}} (\mu\text{m}^2/\text{s})$ | 50.00 | 50.00 ± 0.19 |
| | $k_{\text{off,red}} (1/\text{s})$ | 10.00 | 9.98 ± 0.27 |
| | $k_{\text{off,green}} (1/\text{s})$ | 10.00 | 10.37 ± 0.26 |
| Complex formation and binding | $D_{\text{complex}} (\mu\text{m}^2/\text{s})$ | 39.00 | 38.03 ± 1.63 |
| | $k_{\text{off,complex}} (1/\text{s})$ | 10.00 | 11.78 ± 0.75 |

Errors in ACF or CCF analyses represent the standard error recovered obtained from 25 independent runs.

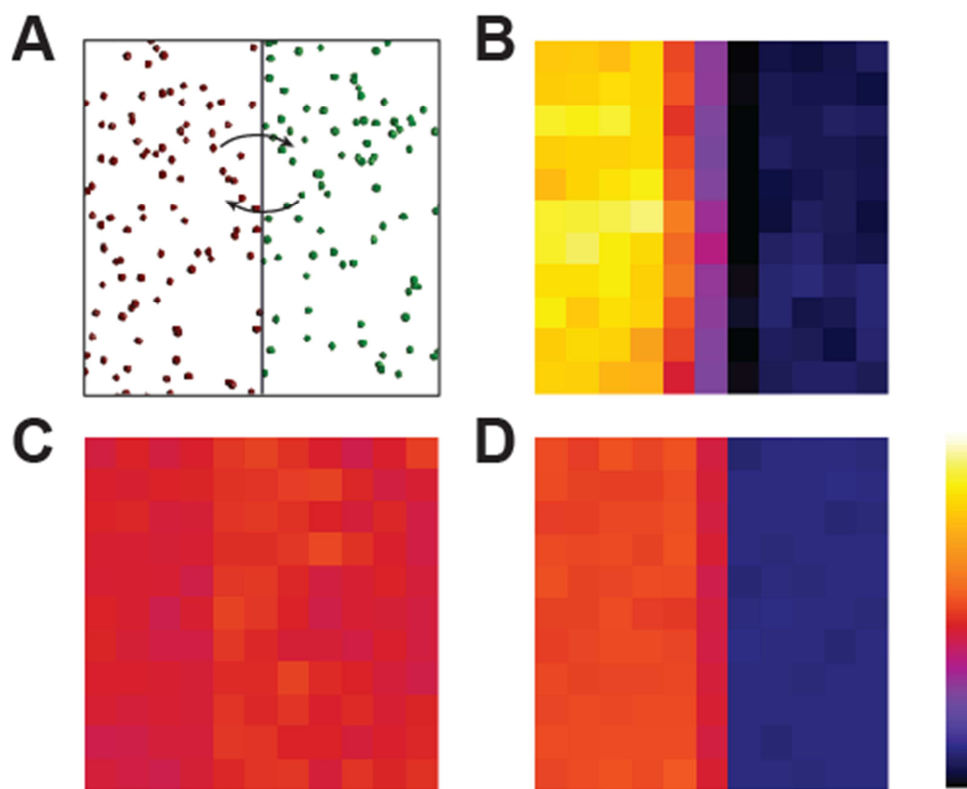


FIGURE S1 Multiplexing point-FCS measurements. The simulation space was considered as a cube divided into two compartments; a 2D scheme of this space is showed in (A). 385 molecules were released in each compartment ($D=40 \mu\text{m}^2/\text{s}$, $\epsilon = 1 \text{ cpm}$ left side, $D=10 \mu\text{m}^2/\text{s}$, $\epsilon = 0.2 \text{ cpm}$ right side) and the simulation was run with $t_s = 10 \mu\text{s}$ during 5 s. The kinetic constant of the molecular conversion at the membrane was set to 10^9 s^{-1} . FERNET was set to collect the intensity traces in an array of 11×11 PSF. Equation 3 was fitted to the ACF calculated at each position to obtain pseudo-color maps of the diffusion coefficients (B) and number of molecules in the confocal volume (C). PCH analysis was performed at each position obtaining a pseudo-color map of brightness (D). Color-code bar represents D values from 8 to $60 \mu\text{m}^2/\text{s}$; N values from 1 to 5 and ϵ values from 0 to 2 cpm (black to white), respectively.

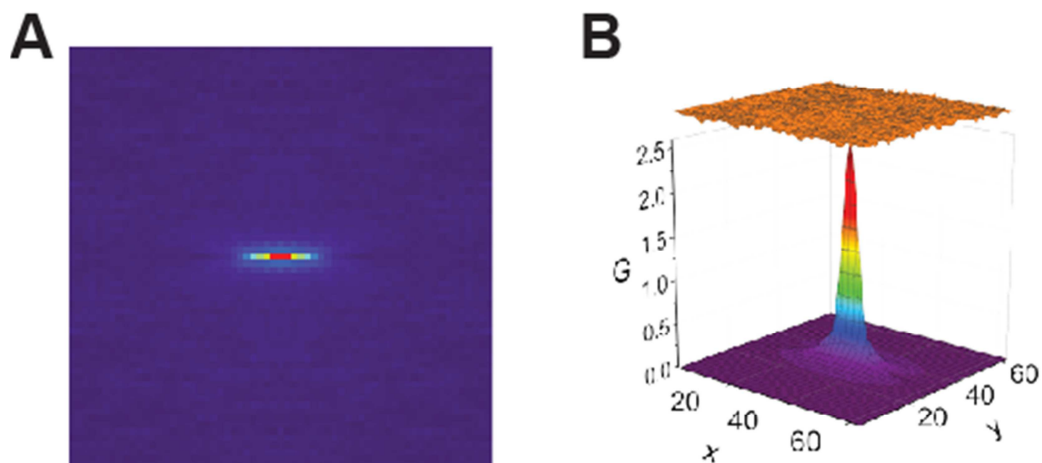


FIGURE S2 Raster image correlation spectroscopy. A similar simulation system to that described in Fig. 1 was considered and FERNET was set to a raster-scan mode. The RICS matrix was calculated from the simulated images (A) and was fitted as described in the text obtaining the best-fit surface (B) and the parameters presented in Table I. Top panel: residuals obtained from the fit.

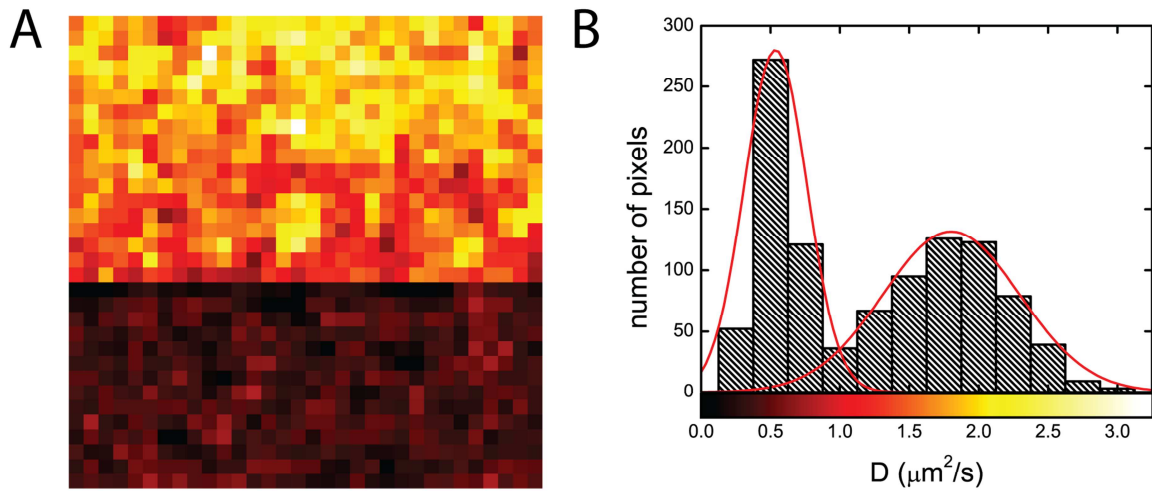


FIGURE S3 Simulations of SPIM-FCS (single plane illumination microscopy in combination with FCS). The simulation scenario was a cube divided into two compartments containing $24 \text{ particles}/\mu\text{m}^3$ each ($D=2 \mu\text{m}^2/\text{s}$, $\epsilon = 1 \text{ cpm}$ top side, $D=0.5 \mu\text{m}^2/\text{s}$, $\epsilon = 1 \text{ cpm}$ bottom side). The kinetic constant of the molecular conversion at the membrane was set to 10^9 s^{-1} . The illumination profile was considered uniform along the x-y plane and Gaussian (waist = $0.5 \mu\text{m}$) in the perpendicular axis (1). MCell was run for $2 \cdot 10^6$ iterations and FERNET was set to simulate intensity traces in SPIM-FCS mode with a frame acquisition time of 1ms. The fluorescence emission was spatially binned to a pixel size of $0.24 \mu\text{m}$, shot noise and Gaussian readout noise ($\sigma = 5$) was added to each pixel. The obtained image stack was processed with the imFCS plugin for ImageJ (2) to obtain the diffusion coefficient map (A, color code in panel B) and its corresponding histogram (B). This data was fitted with a bimodal Gaussian equation (red lines) recovering the following diffusion coefficients: $0.53 \pm 0.32 \mu\text{m}^2/\text{s}$ and $1.80 \pm 0.68 \mu\text{m}^2/\text{s}$ (mean \pm sd).

Supplementary File 1: User manual of FERNET toolkit.

Supplementary File 2: Parameters used for the simulations presented in Fig. 3

MOVIE S1: Simulating confocal imaging. MCell-Blender was programmed to simulate a complex geometrical model in which green fluorescent molecules are covalently bound to a filamentous structure (e.g. a microtubule), and red fluorescent molecules diffuse freely on the simulated space and can attach to the filamentous structure and diffuse over it (e.g. microtubule associated proteins). FERNET was set to perform the raster-scan image acquisition in dual channel mode to simulate images acquired for this scenario in a confocal microscope.

Supplementary references

1. Wohland, T., X. Shi, J. Sankaran, and E. H. Stelzer. 2010. Single plane illumination fluorescence correlation spectroscopy (SPIM-FCS) probes inhomogeneous three-dimensional environments. *Opt Express* 18:10627-10641.
2. Sankaran, J., X. Shi, L. Y. Ho, E. H. Stelzer, and T. Wohland. 2010. ImFCS: a software for imaging FCS data analysis and visualization. *Opt Express* 18:25468-25481.